approach). Nonetheless, the computational costs are manageable given modern computing standards, and would only become prohibitive when an exceedingly large number of additional calibration matrices is used (this should rarely be necessary; for the example considered in this correspondence, the most computationally intensive step of computing $\hat{\mathrm{M}}$ when $N = 6$ takes less than 12 ms in Matlab).

V. Conclusion

An array calibration technique using multiple calibration matrices with angle dependent spherical harmonic correction terms was developed. Results on experimental data show that significant performance gains are achieved with the inclusion of multiple calibration matrices compared to the calibration techniques [1] proposed earlier.

Acknowledgment

The author would like to thank Dr. C. Keller and Dr. G. Hatke for the experimental data used in this correspondence.

References

[1] H. Mir *et al.*, "Self-calibration of an airborne array," *Proc. 38th Asilomar Conf. Signals, Syst. Comput.*, pp. 2340–2344, Nov. 2004.

[2] B. Friedlander and A. J. Weiss, "Direction finding in the presence of mutual coupling," *IEEE Trans. Ant. Propag.*, vol. AP-39, no. 3, pp. 273–284, Mar. 1991.

[3] A. J. Weiss and B. Friedlander, "Effects of modeling errors on the resolution threshold of the MUSIC algorithm," *IEEE Trans. Signal Process.*, vol. 42, no. 6, pp. 1519–1526, Jun. 1994.

[4] B. C. Ng and C. See, "Sensor-array calibration using a maximum-likelihood approach," *IEEE Trans. Ant. Propag.*, vol. 44, no. 6, pp. 827–835, Jun. 1996.

[5] J. Pierre and M. Kaveh, "Experimental performance of calibration and direction-finding algorithms," *Proc. Int. Conf. Acoustics, Speech, Signal Processing (ICASSP)*, pp. 1365–1368, May 1991.

[6] D. Fuhrmann and D. Rieken, "Array calibration for circular-array STAP using clutter scattering and projection matrix fitting," in *Proc. Adaptive Sensor Array Processing Workshop (ASAP)*, Mar. 2000, pp. 79–84.

[7] L. Trefethen and D. Bau, *Numerical Linear Algebra*. Philadelphia, PA: SIAM, 1997.

[8] E. Hobson, *The Theory of Spherical and Ellipsoidal Harmonics*. New York: Chelsea, 1955.

[9] W. Stutzman and G. Thiele, *Antenna Theory and Design*. New York: Wiley, 1997.

[10] H. Van Trees, *Optimum Array Processing (Detection, Estimation, and Modulation Theory, Part IV)*. New York: Wiley-Interscience, 2002.

[11] Q. Bao, C. Ko, and W. Zhi, "DOA estimation under unknown mutual coupling and multipath," *IEEE Trans. Aerosp. Electron. Syst.*, vol. 41, no. 2, pp. 565–573, 2005.

[12] H. Steyskal and J. Herd, "Mutual coupling compensation in small array antennas," *IEEE Trans. Ant. Propag.*, vol. AP-38, no. 12, pp. 1971–1975, Dec. 1990.

Design of Frequency Invariant Beamformers for Broadband Arrays

Wei Liu, *Member, IEEE*, and Stephan Weiss, *Senior Member, IEEE*

***Abstract*—A new class of broadband arrays with frequency invariant beam pattern is proposed. By suitable substitutions, the beam pattern of a continuous sensor array can be regarded as the Fourier transform of its spatial and temporal parameters. For the design of practical discrete sensor arrays, it can be regarded as an approximation to the continuous sensor case and a simple design method is provided, which can be applied to linear, rectangular and cubic broadband arrays.**

***Index Terms*—Beamforming, frequency-invariant design, multi-dimensional arrays.**

I. Introduction

In the past, broadband beamformers have been studied extensively due to their applications to sonar, radar, and communications [1], [2]. Amongst them is a class of arrays with frequency invariant responses, which can achieve a beam pattern independent of frequency, therefore with a constant beamwidth.

The design of the frequency-invariant beamformer can be achieved by direct optimization for all of the coefficients with respect to the desired response using the available covex programming optimization methods [3]–[6], but for large linear/planar arrays, the number of coefficients to be optimized will be extremely large. Harmonic nesting is a widely used method [7]–[10] and although the resulting beampattern is octave independent, the spatial resolution within an octave band is still dependent on frequency. In [11], constant beamwidth multibeam is achieved by superimposing several marginally steered beams. Different from the above methods, an approach employing the asymptotic theory of unequally spaced arrays has been suggested in [12], where the relationship between the beam pattern properties and array properties is derived and exploited for the broadband linear array design. Most of the above work is focused on linear arrays, and recently the design of the frequency-invariant beamformer for circular arrays has also been studied [13] and then extended to the case of concentric circular arrays [14] and concentric spherical arrays [15]. Instead of focusing on one basic type of arrays, a systematic method has been proposed in [16], which can be applied to one-dimensional (1–D), two-dimensional (2–D), and three-dimensional (3–D) arrays. In this new method, each element of the array is followed by its own primary filter, and the outputs of these primary filters share a common secondary filter to form the final output. Although the design for a 1–D array is relatively simple because of the dilation property of the primary filters, for higher dimensional arrays this property is not guaranteed, which makes the general design case too complicated, and no design examples for a 2–D array were provided there.

Manuscript received August 31, 2006; revised June 28, 2007. The associate editor coordinating the review of this manuscript and approving it for publication was Prof. Daniel Fuhrmann. This work was supported by the Nuffield Foundation award NAL/32599 for newly appointed lecturers.

W. Liu is with the Communications Research Group, Department of Electronic and Electrical Engineering, University of Sheffield, Sheffield S1 3JD, U.K. (e-mail: w.liu@sheffield.ac.uk).

S. Weiss is with the Institute for Communications and Signal Processing, School of Electronic and Electrical Engineering, University of Strathclyde, Glasgow G1 1XW, U.K. (e-mail: stephan.weiss@eee.strath.ac.uk).

Digital Object Identifier 10.1109/TSP.2007.907872

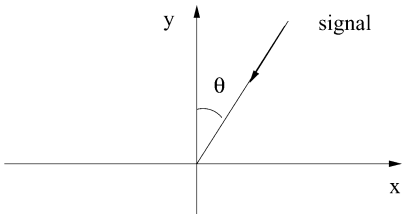

Fig. 1. Continuous sensor array aligned with the x axis.

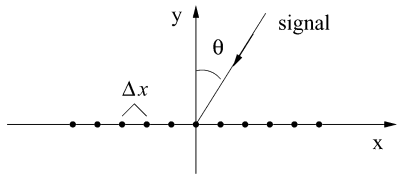

Fig. 2. Equally spaced linear array with a sensor spacing of Δx, where the signal impinges from the direction θ.

In this correspondence, we propose a new class of broadband arrays with frequency invariant beam patterns, which exploits the Fourier transform relationship between the array's spatial and temporal parameters and its beam pattern [17] and can be applied to linear (1–D), rectangular (2–D), and cubic (3–D) arrays. Starting from the desired frequency-invariant beam pattern of an n-D array, the proposed method uses a series of substitutions and an n-D inverse Fourier transform to achieve a frequency-invariant beamformer design. Two design examples—one for a linear array and one for a planar array—are given to highlight its effectiveness. A previously proposed frequency-invariant linear array [18] with tapped delay lines can be regarded as a special case of this new class of arrays.

This correspondence is organized as follows. Section II addresses the design problem with continuous sensors first, then the case with discrete sensor arrays is discussed as an approximation to the ideal continuous sensor case. Thereafter, a systematic design procedure is derived. Two design examples are given in Section III and conclusions drawn in Section IV.

II. Frequency-Invariant Beamforming

A. One-Dimensional Array

Fig. 1 shows a one-dimensional continuous sensor array aligned with the x axis, where a planar wave with angular frequency ω illuminates the array from an angle θ measured from broadside. Its beam response is given by

$$P(\omega,\theta)=\int_{-\infty}^{\infty} e^{-j\frac{\omega\sin\theta}{c}x}D(x,\omega)dx \tag{1}$$

where c is the propagation speed and $D(x,\omega)$ is the frequency response of the sensor at location x. By substitution $\omega_1=(\omega\sin\theta/c)$, we have

$$P(\omega_1,\omega)=\int_{-\infty}^{\infty} e^{-j\omega_1 x}D(x,\omega)dx. \tag{2}$$

From (2), it is clear that $P(\omega,\theta)$ can be obtained by first applying a 1–D Fourier transform to $D(x,\omega)$ and then resubstituting $\omega_1=(\omega\sin\theta/c)$.

For the beam pattern to be frequency invariant, $P(\omega_1,\omega)$ must be a function of only θ, or more precisely $\sin\theta$. Let $F(\sin\theta)$ be such a frequency invariant beam pattern. In order to match this desired beam pattern, $P(\omega_1,\omega)$ must, after resubstituting $\omega_1=(\omega\sin\theta/c)$, be identical to $F(\sin\theta)$. In order to achieve this, the variables ω_1 and ω must obey a specific dependency in the expression of $P(\omega_1,\omega)$ for ω to disappear. Note that if $P(\omega_1,\omega)$ is a function of $c(\omega_1/\omega)$, then after the resubstitution, $c(\omega_1/\omega)$ will change to

$$c\frac{\omega_1}{\omega}=c\frac{\omega\sin\theta}{c\omega}=\sin\theta \tag{3}$$

thus eliminating any dependency on ω. Therefore, we can set $P(\omega_1,\omega)=F(\omega_1 c/\omega)$ for a desired frequency-invariant beam pattern $F(\sin\theta)$.

Based on the above analysis, the idea of designing a frequency invariant beamformer can be summarized as follows. Given a desired frequency-invariant beam pattern $F(\sin\theta)$, which can be any function of $\sin\theta$, with any shape, and can be obtained by a narrowband beamformer design method, we set $P(\omega_1,\omega)=F(\omega_1 c/\omega)$. Applying an inverse Fourier transform to $P(\omega_1,\omega)$ with respect to the variable ω_1, we obtain the desired frequency response $D(x,\omega)$ for any position x. $D(x,\omega)$ can then be realized by either an analog filter or digital filter, which can be obtained by an appropriate filter design method.

A continuous sensor is an ideal situation. In practice we can only have sensors at specific positions. For a uniformly spaced linear array with adjacent sensor spacing of Δx, as shown in Fig. 2, the integration in (1) changes to summation

$$P(\omega,\theta)=\sum_{m=-\infty}^{\infty} D(m\Delta x,\omega)e^{-j\frac{\omega\sin\theta m\Delta x}{c}}. \tag{4}$$

With $\omega_1=(\omega\sin\theta\Delta x/c)$, we have

$$P(\omega_1,\omega)=\sum_{m=-\infty}^{\infty} D(m\Delta x,\omega)e^{-jm\omega_1}. \tag{5}$$

In order to avoid aliasing, $\Delta x<\lambda_{\min}/2$, where $\lambda_{\min}$ is the wavelength of the maximum frequency of interest $\omega_{\max}$. Based on the discussion in the continuous sensor case, the design of this discrete sensor case can be described as follows.

- **Step 1**. Given a desired frequency-invariant beam pattern $F(\sin\theta)$, and the substitution $\sin\theta=(\omega_1 c/\omega\Delta x)$

$$P(\omega_1,\omega)=\begin{cases}F\left(\frac{c\omega_1}{\omega\Delta x}\right) & \text{for } |\omega_1|\le\left|\frac{\omega\Delta x}{c}\right|\wedge\omega\in[\omega_{\min};\omega_{\max}]\\ A(\omega_1) & \text{for otherwise}\end{cases} \tag{6}$$

is obtained for $\omega_1\in[-\pi;\pi)$, where $\omega_{\min}$ is the minimum frequency of interest and $A(\omega_1)$ is an arbitrary function with finite values. As the Fourier transform of $D(m\Delta x,\omega)$, $P(\omega_1,\omega)$ should be a periodic function with a period of 2π. For $\omega_1\in[-\pi;\pi)$, since $|\sin\theta|\le 1$, $F(c\omega_1/\omega\Delta x)$ is only defined on the shaded area shown in Fig. 3. For the remaining area, the value of $P(\omega_1,\omega)$, i.e., $A(\omega_1)$, can be modified arbitrarily without affecting the resultant beam pattern in theory. This is also the so-called "nonvisible region" in [4]. However, the choice of $A(\omega_1)$ can affect the smoothness of the function $P(\omega_1,\omega)$ over the whole area of $\omega_1\in[-\pi;\pi)$ and since in the next step we will perform an inverse Fourier transform to $P(\omega_1,\omega)$ and then truncate the result, it will affect the number samples required to represent the response of the function $P(\omega_1,\omega)$ within some error. As a result, it will indeed affect the resultant beam pattern for a finite number of array sensors. Therefore, the choice of

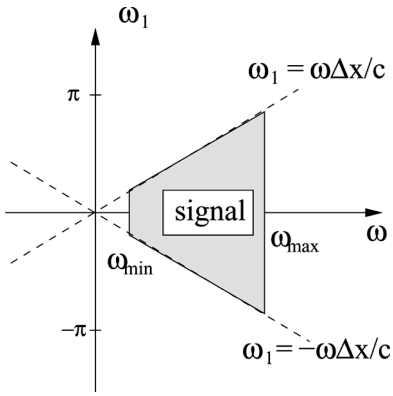

Fig. 3. Shaded area defined by $|\omega_1| \leq |(\omega\Delta x/c)| \wedge \omega \in [\omega_{\min}; \omega_{\max}]$ for $F(c\omega_1/\omega\Delta x)$.

$A(\omega_1)$ should aim to generate a function $P(\omega_1, \omega)$ as smooth as possible, and in the design example, we simply choose it to be zero for the whole defined area.

- **Step 2**. Applying the 1–D inverse Fourier transform (IFT) to $P(\omega_1, \omega)$ with respect to the variable ω_1, we can get the desired frequency responses $D(m\Delta x, \omega)$ for the sensor at a position of $m\Delta x$, $m = \ldots, -1, 0, 1, \ldots$. Suppose the sensor number is M. $D(m\Delta x, \omega)$ can be obtained by the inverse discrete Fourier transform (IDFT) as an approximation, by sampling $P(\omega_1, \omega)$ on the $\tilde{M} > M$ points of $\omega_1 = -\pi + 2\tilde{m}\pi/\tilde{M}$, $\tilde{m} = 0, 1, \ldots, \tilde{M} - 1$. Then, $D(\tilde{m}\Delta x, \omega)$ can be obtained easily by the $\tilde{M}$-point IDFT of $P(-\pi + 2\tilde{m}\pi/\tilde{M}, \omega)$. To fit the real dimension M of the array, we need to truncate the resultant $D(m\Delta x, \omega)$ to the size of M, with an appropriate window function, such as a rectangular window or a hamming window.

The approach outlined above can be applied to any desired frequency-invariant beam pattern $F(\sin\theta)$.

B. Two-Dimensional Array

Fig. 4 shows a 2–D continuous sensor array in the (x, y) plane. Its beam response is given by

$$P(\omega, \theta, \phi) = \int\int_{-\infty}^{\infty} e^{-j\frac{\omega}{c}(x\sin\theta\cos\phi + y\sin\theta\sin\phi)} \cdot D(x, y, \omega)dxdy \tag{7}$$

where $D(x, y, \omega)$ is the frequency response of the sensor at the point (x, y). The substitutions $\omega_1 = ((\omega\sin\theta\cos\phi)/c)$ and $\omega_2 = ((\omega\sin\theta\sin\phi)/c)$ into (7) result in

$$P(\omega_1, \omega_2, \omega) = \int\int_{-\infty}^{\infty} D(x, y, \omega) e^{-j\omega_1 x} e^{-j\omega_2 y} dxdy \tag{8}$$

i.e., $P(\omega_1, \omega_2, \omega)$ is the 2–D Fourier transform of $D(x, y, \omega)$. If this Fourier transfrom can be expressed as $P(\omega_1, \omega_2, \omega) = F((\omega_1 c)/\omega), ((\omega_2 c)/\omega))$, where $F(\hat{\omega}_1, \hat{\omega}_2)$ is the frequency response

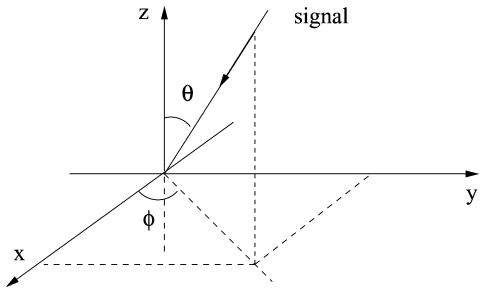

Fig. 4. Continuous 2–D sensor array, where the signal impinges from the direction (θ, ϕ).

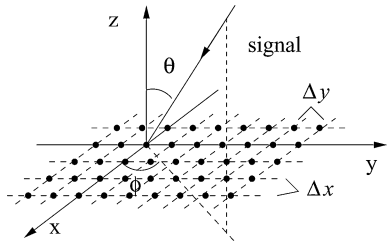

Fig. 5. Equally spaced planar array with sensor spacings of Δx and Δy respectively, where the signal impinges from the direction (θ, ϕ).

of a 2–D filter with $\hat{\omega}_1$ and $\hat{\omega}_2$ representing the two corresponding frequency variables, then the resulting function $F(\sin\theta\cos\phi, \sin\theta\sin\phi)$ will represent the frequency invariant beam pattern.

Suppose $F(\sin\theta\cos\phi, \sin\theta\sin\phi)$ is the desired beam pattern. We set $P(\omega_1, \omega_2, \omega) = F((\omega_1 c)/\omega, (\omega_2 c)/\omega)$. Applying a 2–D inverse Fourier transform to $P(\omega_1, \omega_2, \omega)$ with respect to the variables ω_1 and ω_2, we then obtain the desired frequency response $D(x, y, \omega)$ for any position (x, y).

Now, consider the uniformly spaced discrete sensor case, as shown in Fig. 5. Then, (7) changes to

$$P(\omega, \theta, \phi) = \sum_{l,m=-\infty}^{\infty} D(l\Delta x, m\Delta y, \omega) \times e^{-j\frac{\omega(l\Delta x\sin\theta\cos\phi + m\Delta y\sin\theta\sin\phi)}{c}} \tag{9}$$

and

$$P(\omega_1, \omega_2, \omega) = \sum_{l,m=-\infty}^{\infty} D(l\Delta x, m\Delta y, \omega) \times e^{-jl\omega_1} e^{-jm\omega_2} \tag{10}$$

with $\omega_1 = (\omega\sin\theta\cos\phi\Delta x/c)$ and $\omega_2 = (\omega\sin\theta\sin\phi\Delta y/c)$. To avoid aliasing, $\Delta x, \Delta y < \lambda_{\min}/2$. Analogous to the 1-D design in Section II-A, the 2–D frequency invariant beamformer can be designed as follows.

- **Step 1**. With the substitutions $\sin\theta\cos\phi = c\omega_1/\omega\Delta x$ and $\sin\theta\sin\phi = c\omega_2/\omega\Delta y$, we obtain $P(\omega_1, \omega_2, \omega)$ defined over one period $\omega_1, \omega_2 \in [-\pi; \pi)$ as (11), shown at the bottom of the page, where $A(\omega_1, \omega_2)$ is an arbitrary function with finite values, and also defined on the nonvisible region as $A(\omega_1)$ in the 1–D

$$P(\omega_1, \omega_2, \omega) = \begin{cases} F(\frac{c\omega_1}{\omega\Delta x}, \frac{c\omega_2}{\omega\Delta y}), & \text{for } (\frac{c\omega_1}{\omega\Delta x})^2 + (\frac{c\omega_1}{\omega\Delta y})^2 \leq 1 \wedge \omega \in [\omega_{\min}; \omega_{\max}] \\ A(\omega_1, \omega_2), & \text{for otherwise} \end{cases} \tag{11}$$

design case. Its choice should also aim to generate a smoother function $P(\omega_1, \omega_2, \omega)$.

- **Step 2**. Applying a 2–D inverse Fourier transform to $P(\omega_1, \omega_2, \omega)$ with respect to the two variables ω_1 and ω_2 returns the desired frequency response $D(l\Delta x, m\Delta y, \omega)$ for the corresponding sensors. Suppose the sensor number is $L \times M$. As an approximation, we can employ the 2–D IDFT by sampling $P(\omega_1, \omega_2, \omega)$ on the $\tilde{L} \times \tilde{M}$ points of $\omega_1 = -\pi + (2\tilde{l}\pi/\tilde{L}), \tilde{l} = 0, 1, \ldots, \tilde{L} - 1$, and $\omega_2 = -\pi + (2\tilde{m}\pi/\tilde{M}), \tilde{m} = 0, 1, \ldots, \tilde{M} - 1$, where $\tilde{L} > L$ and $\tilde{M} > M$. To fit the real dimension $L \times M$ of the array, we need to truncate the resultant $D(l\Delta x, m\Delta y, \omega)$ to the size of $L \times M$, with an appropriate window function.

C. Three-Dimensional Array

The response of a 3–D continuous sensor array, which in addition to Fig. 4 also extends in z direction, is given by

$$P(\omega, \theta, \phi) = \int\int\int_{-\infty}^{\infty} D(x, y, z, \omega) e^{-j\frac{\omega \sin\theta\cos\phi}{c}x} \times e^{-j\frac{\omega \sin\theta\sin\phi}{c}y} e^{-j\frac{\omega\cos\theta}{c}z} dxdydz. \quad (12)$$

Here, the substitutions $\omega_1 = (\omega \sin\theta\cos\phi/c)$, $\omega_2 = (\omega \sin\theta \sin\phi/c)$, and $\omega_3 = (\omega\cos\theta/c)$ lead to

$$P(\omega_1, \omega_2, \omega_3, \omega) = \int\int\int_{-\infty}^{\infty} D(x, y, z, \omega) e^{-j\omega_1 x} e^{-j\omega_2 y} e^{-j\omega_3 z} dxdydz. \quad (13)$$

For a uniformly spaced 3–D array with spacings of $\Delta x, \Delta y$ and Δz, (12) changes to

$$P(\omega, \theta, \phi) = \sum_{k,l,m=-\infty}^{\infty} D(k\Delta x, l\Delta y, m\Delta z, \omega) \times e^{-j\frac{k\omega \sin\theta\cos\phi\Delta x}{c}} e^{-j\frac{l\omega\sin\theta\sin\phi\Delta y}{c}} e^{-j\frac{m\omega\cos\theta\Delta z}{c}}. \quad (14)$$

Based on this, we can develop a similar design method as in Sections II-A and II-B, and it is omitted here.

III. Design Examples

We provide two examples for the design of a frequency invariant beamformer with potential applications to microphone arrays. The frequency range of interest is set to be $0 < f \leq 12$ kHz and the propagation speed is 340 m/s. The first example is for a linear array with 21 sensors and the second one for a planar array with 21×21 sensors, both with an adjacent sensor spacing of $(340 \text{ m/s})/(2 \times 12 \text{ kHz}) = 1.42$ cm. The desired beam pattern for the linear array is given by

$$F_{1D}(\sin\theta) = \sum_{m=-3}^{3} h_m e^{-jm\pi\sin\theta} \quad (15)$$

where the coefficients $\{h_{-3}, h_{-2}, \ldots, h_2, h_3\}$ are obtained by the filter design program remez provided by Matlab, their values are, respectively

$$\{h_m\} = [0.0307\ 0.2028\ 0.1663\ 0.2004\ 0.1663\ 0.2028\ 0.0307]. \quad (16)$$

They form a desired equiripple frequency-invariant response.

We employed a 64-point 1–D IDFT on the resultant periodic function $P(\omega_1, \omega)$ and set $P(\omega_1, \omega) = 0$ for the area where there is no signal existing, as indicated in Step 1 of the 1–D array design. The resultant 64 desired frequency responses $D(m\Delta x, \omega)$, with each corresponding to an analog or digital filter following each of the 21 sensors, were then truncated to the size of 21 directly, with a rectangular window. Given the 21 desired frequency responses $D(m\Delta x, \omega), m = -10, \ldots, 1, 0, 1, \ldots, 10$, we can employ an appropriate filter design method to design 21 analog or digital filters to realize them. The magnitude responses $|D(m\Delta x, \omega)|$ are shown in Fig. 6 to give a rough idea about the design results. As the filter design problem is not the focus of this correspondence, we assumed that the 21 filters had been obtained with the desired frequency responses $D(m\Delta x, \omega)$ (the same assumption for the planar array design) and then used $D(m\Delta x, \omega)$ to calculate the resultant beam pattern, which is shown in Fig. 7 with a clear frequency invariant property except for very low frequencies. For lower frequencies, the array aperture becomes relatively small and in the extreme case, for the dc component (zero frequency), the array will not be able to form any beam. This is a limitation inherent to all kinds

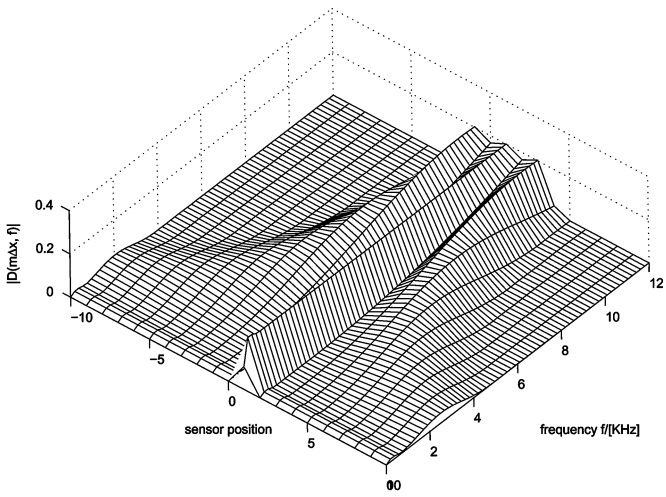

Fig. 6. Desired magnitude responses $|D(m\Delta x, f)|$ of the 21 filters in frequency domain for the linear array design result.

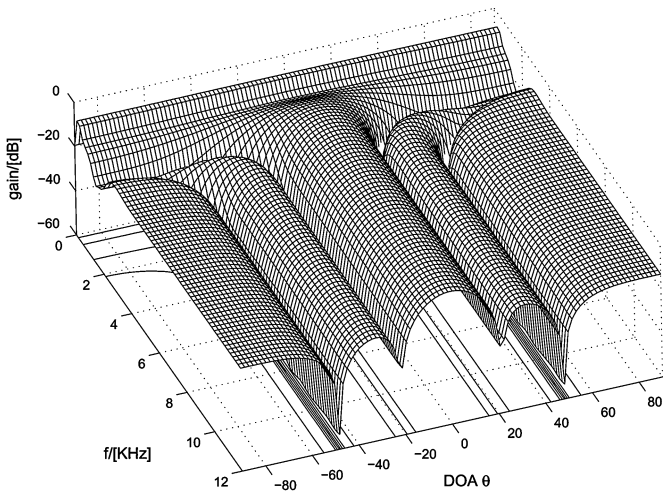

Fig. 7. Resultant frequency invariant beam pattern for the linear array design.

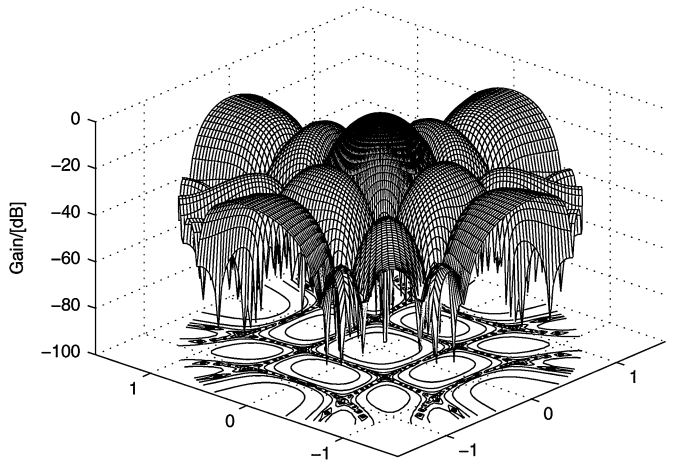

Fig. 8. Resultant beam pattern of the planar array at $f = 7.2$ kHz.

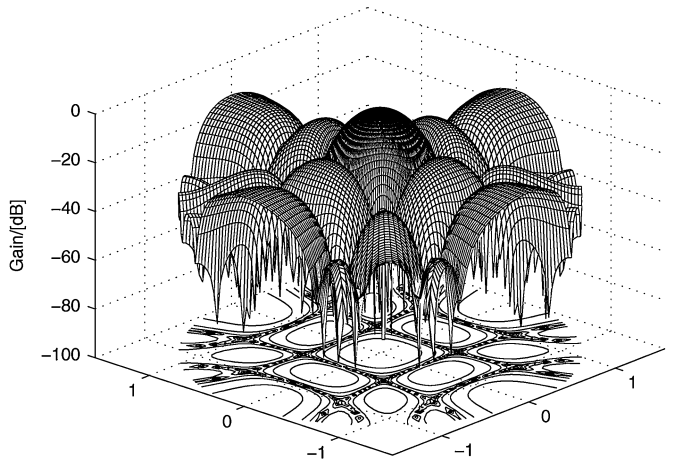

Fig. 9. Resultant beam pattern of the planar array at $f = 9.6$ kHz.

of beamforming system. To extend the frequency invariant property to a lower frequency, there are three solutions: the first one is to increase the number of array sensors; the second one is to reduce the complexity of the desired beam pattern (with a wider beamwidth and higher sidelobe level); the third one is to reduce the upper frequency boundary and increase the array sensor spacing. In the design example, the upper frequency boundary is 12 kHz and the spacing is 1.42 cm. We can reduce this boundary to 4 kHz and increase the spacing to $(340\ \text{m/s})/(2 \times 4\ \text{kHz}) = 4.25$ cm, and the resultant beam pattern will be the same as the one shown in the design. In this case, the lower frequency boundary with frequency invariant property will be reduced accordingly, which will be lower than 1 kHz.

For the second design example, the desired beam pattern is given by

$$F_{2D}(\sin\theta\cos\phi, \sin\theta\sin\phi) = \frac{1}{25}\sum_{l=-2}^{2}\sum_{m=-2}^{2} e^{-jl\pi\sin\theta\cos\phi} e^{-jm\pi\sin\theta\sin\phi}. \quad (17)$$

According to (11), we first obtained the response $P(\omega_1, \omega_2, \omega)$ with $A(\omega_1, \omega_2) = 0$. A 64×64 2–D IDFT was employed, and the 64×64 desired frequency responses $D(l\Delta x, m\Delta y, \omega)$ were then subsequently truncated to the intended array dimension of 21×21. The resultant beam pattern is four-dimensional, and here we can only provide some

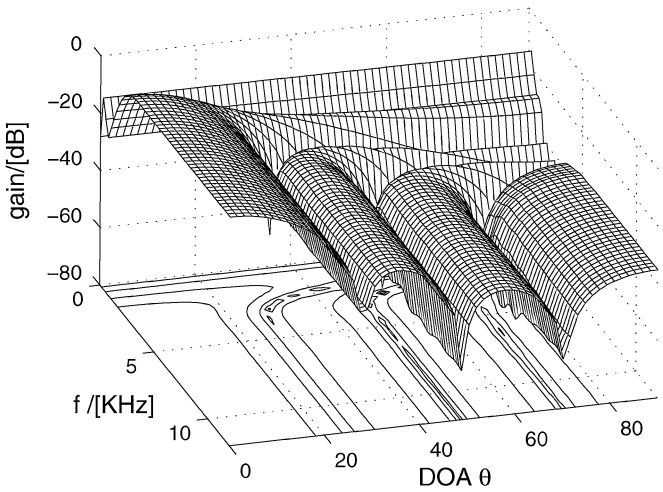

Fig. 10. Slice of the beam pattern at $\phi = 60°$.

exemplary snapshots. Figs. 8 and 9 are the array's response in a cylindrical coordinates to the frequencies $f = 7.2$ kHz and $\omega = 9.6$ kHz, respectively. The height axis is the magnitude response of the beam, the radial coordinate is for the elevation angle θ and the angle coordinate is for the azimuth angle ϕ. The frequency invariant property can be verified by the similarity of these two figures, and further shown by a slice of its beam pattern at $\phi = 60°$, as given in Fig. 10.

IV. Conclusion

A new class of broadband arrays with frequency invariant beam patterns has been proposed, which was derived by first studying the ideal continuous sensor case and then extending the idea to the practical case with discrete sensors. The proposed design can be applied to linear, rectangular and cubic arrays and the design results are the desired frequency responses of the filters following each of the sensors and can be realized by either an analogue filter or a digital filter. Two design examples have been provided, yielding satisfactory frequency invariant characteristics over a large range of frequencies.

References

[1] H. L. Van Trees, *Optimum Array Processing, Part IV of Detection, Estimation, and Modulation Theory*. New York: Wiley, 2002.

[2] M. Ghavami, L. B. Michael, and R. Kohno, *Ultra Wideband Signals and Systems in Communication Engineering*. Chichester, U.K.: Wiley, 2004.

[3] D. P. Scholnik and J. O. Coleman, "Optimal design of wideband array patterns," in *Proc. IEEE Int. Radar Conf.*, Washington, DC, May 2000, pp. 172–177.

[4] D. P. Scholnik and J. O. Coleman, "Formulating wideband array-pattern optimizations," in *Proc. IEEE Int. Conf. Phased Array Systems Technology*, Dana Point, CA, May 2000, pp. 489–492.

[5] D. P. Scholnik and J. O. Coleman, "Superdirectivity and SNR constraints in wideband array-pattern design," in *Proc. IEEE Int. Radar Conf.*, Atlanta, GA, May 2001, pp. 181–186.

[6] S. F. Yan and Y. L. Ma, "Design of FIR beamformer with frequency invariant patterns via jointly optimizing spatial and frequency responses," in *Proc. IEEE Int. Conf. Acoustics, Speech, Signal Processing*, Philadelphia, PA, Mar. 2005, pp. 789–792.

[7] R. Smith, "Constant beamwidth receiving arrays for broad band sonar systems," *Acustica*, vol. 23, pp. 21–26, 1970.

[8] E. L. Hixson and K. T. Au, "Widebandwidth constant beamwidth acoustic array," *J. Acoust. Soc. Amer.*, vol. 48, no. 1, p. 117, Jul. 1970.

[9] T. Chou, "Frequency-independent beamformer with low response error," in *Proc. IEEE Int. Conf. Acoustics, Speech, Signal Processing*, Detroit, MI, May 1995, vol. 5, pp. 2995–2998.

[10] S. Weiss, R. W. Stewart, and W. Liu, "A broadband adaptive beamformer in subbands with scaled aperture," in *Proc. Asilomar Conf. Signals, Systems, Computers*, Monterey, CA, Nov. 2002, pp. 1298–1302.
[11] M. M. Goodwin and G. W. Elko, "Constant beamwidth beamforming," in *Proc. IEEE Int. Conf. Acoustics, Speech, Signal Processing*, Minneapolis, MN, Apr. 1993, vol. 1, pp. 169–172.
[12] J. H. Doles, III and F. D. Benedict, "Broad-band array design using the asymptotic theory of unequally spaced arrays," *IEEE Trans. Antennas Propag.*, vol. 36, pp. 27–33, Jan. 1988.
[13] S. C. Chan and K. S. Pun, "On the design of digital broadband beamformer for uniform circular array with frequency invariant characteristics," in *Proc. IEEE Int. Symp. Circuits Systems*, Phoenix, AZ, May 2002, vol. 1, pp. 693–696.
[14] S. C. Chan and H. H. Chen, "Theory and design of uniform concentric circular arrays with frequency invariant characteristics," in *Proc. IEEE Int. Conf. Acoust., Speech, Signal Processing*, Philadelphia, PA, Mar. 2005, vol. 4, pp. 805–808.
[15] S. C. Chan and H. H. Chen, "Theory and design of uniform concentric spherical arrays with frequency invariant characteristics," in *Proc. IEEE Int. Conf. Acoustics, Speech, Signal Processing*, Toulouse, France, May 2007, vol. IV, pp. 1057–1060.
[16] D. B. Ward, R. A. Kennedy, and R. C. Williamson, "Theory and design of broadband sensor arrays with frequency invariant far-field beam patterns," *J. Acoust. Soc. Amer.*, vol. 97, no. 2, pp. 1023–1034, Feb. 1995.
[17] S. Haykin and J. Kesler, "Relation between the radiation pattern of an array and the two-dimensional discrete Fourier transform," *IEEE Trans. Antennas Propag.*, vol. AP-23, no. 3, pp. 419–420, May 1975.
[18] T. Sekiguchi and Y. Karasawa, "Wideband beamspace adaptive array utilizing FIR fan filters for multibeam forming," *IEEE Trans. Signal Process.*, vol. 48, no. 1, pp. 277–284, Jan. 2000.

On the Deterministic CRB for DOA Estimation in Unknown Noise Fields Using Sparse Sensor Arrays

Martin Kleinsteuber and Abd-Krim Seghouane, *Member, IEEE*

***Abstract*—The Cramér–Rao bound (CRB) plays an important role in direction of arrival (DOA) estimation because it is always used as a benchmark for comparison of the different proposed estimation algorithms. In this correspondence, using well-known techniques of global analysis and differential geometry, four necessary conditions for the maximum of the log-likelihood function are derived, two of which seem to be new. The CRB is derived for the general class of sensor arrays composed of multiple arbitrary widely separated subarrays in a concise way via a coordinate free form of the Fisher Information. The result derived in [1] is confirmed.**

***Index Terms*—Cramér–Rao bound (CRB), differential geometry, direction of arrival (DOA) estimation, maximum likelihood.**

I. Introduction

The maximum likelihood technique is a widely used tool for directions of arrival (DOA) estimation. Many log-likelihood functions and estimation algorithms have been proposed in the literature depending on the structure of the noise covariance matrix which make them sensitive to the assumed noise model. In most practical situations, the noise model is unknown and to effectively handle unknown noise environments several methods have been proposed. The most recent one consists of spacing the array geometry in certain ways. In this correspondence, the general case of sensor arrays composed of multiple arbitrary widely separated subarrays [1] is considered. In such arrays, intersubarray spacings are substantially larger than the signal wavelength and the noise covariance matrix of the whole array is block-diagonal.

The classical way for deriving the maximum likelihood estimate of the DOA is by setting the derivative of the log-likelihood function with respect to the DOA parameters to zero and solving the formed equation set. Note, that two different types of data models are used in applications for DOA estimation. The so-called conditional model, where the signal is supposed to be nonrandom, and the unconditional model, where the signal is assumed to be random [2]. Since the results derived in this correspondence are extensions of previous results derived in [1], we exclusively focus on the first case—the conditional model and the corresponding likelihood function.

To assess the performance of these derived maximum likelihood estimators, the Cramér–Rao bound (CRB) plays an important role because it is always used as a benchmark for comparison. The derivation of closed-form expressions for the CRB for the general unknown noise model have been approached in [3]–[5] and obtained for the uniform and nonuniform white noise case in [6] and [7]. An extension of the

Manuscript received December 3, 2006; revised June 18, 2007. The associate editor coordinating the review of this manuscript and approving it for publication was Dr. Andreas Jakobsson. This work was performed at NICTA, Canberra Research Laboratory. National ICT Australia is funded by the Australian Department of Communications, Information Technology and the Arts and the Australian Research Council through Backing Australia's Ability and the ICT Center of Excellence Program.

M. Kleinsteuber was with National ICT Australia Limited, Canberra Research Laboratory, Canberra ACT 2601, Australia. He is now with Mathematisches Institut, 97074 Wurzburg, Germany (e-mail: kleinsteuber@mathematik.uni-wuerzburg.de).

A.-K. Seghouane is with the National ICT Australia, Canberra Research Laboratory, Canberra ACT 2601, Australia, and also with the Research School of Information Sciences and Engineering (RSISE), Australian National University, Canberra, ACT 0200, Australia (e-mail: Abd-krim.seghouane@nicta.com.au).

Digital Object Identifier 10.1109/TSP.2007.907832